

Forcing Level Effects of Internal Acoustic Excitation on the Improvement of Airfoil Performance

R. C. Chang*

CSIST, Taichung, Taiwan, Republic of China

and

F.-B. Hsiao† and R.-N. Shyu‡

National Cheng Kung University, Tainan, Taiwan, Republic of China

The effects of internal acoustic excitation on the leading-edge, separated boundary layers and the aerodynamic performance of NACA 63₃-018 cross section airfoil are examined as a function of forcing level and forcing frequency of the introduced acoustics. Tests are separately conducted in two suction, open-typed wind tunnels at the Reynolds number of 3.0×10^5 for the measurements and 1.0×10^4 for the visualization. Results indicate that the flow separation is delayed at the angles of attack higher than the stalled angle of small level excitation with the forcing frequency f_e near the shear layer instability frequency f_t . As the forcing level is increased to some extent, the velocity fluctuations around the slot exit are demonstrated to be the primary governing parameter for modifying the separated boundary layers. Data also show that the effective forcing frequency (and the Strouhal number, St) extends over wider range as compared to the lower level excitation. Meanwhile, the pressure distributions on the airfoil surface exhibit recovery behaviors with different forcing frequencies. The corresponding boundary layers are visualized to be reattached to the surface to form a recirculation region when the airfoil is around at the stalled angles.

Nomenclature

C	= chord
C_d	= section drag coefficient
C_l	= section lift coefficient
C_p	= pressure coefficient
f_e	= excitation frequency
f_t	= shear layer instability frequency
P	= pressure
St	= Strouhal number, $f_e C/U_\infty$
t	= time
U	= mean velocity in X direction
U_s, V_s	= surface velocity in x, y direction
U_∞	= freestream velocity
u'_{\max}	= maximum value of velocity perturbations
X_a	= asymptotic pressure-recovery point
X, Y	= streamwise and transverse coordinates
x, y	= tangential and normal coordinate to airfoil surface
μ	= viscosity
Ω	= vorticity

Introduction

THE usage of acoustic excitation in the control of flow separation has been well recognized for many decades. It has been found that acoustics at particular frequencies and levels could influence the separated boundary layers about a wing¹⁻⁴ or a cylinder.⁵⁻⁷ The excited flowfield exhibits different behaviors and the momentum exchange is enhanced in the boundary layer close to the surface. Collins and Zelenevitz¹ applied the acoustics "externally" to a high-angle-of-attack (high-AOA) airfoil where the flow was separated. They found

that the externally introduced acoustics could excite the flow to cause a partial reattachment of the separated flow so that the airfoil performance was improved. Similar studies on the effect of external acoustic excitation about a stalled airfoil were also performed by Ahuja et al.² and Zaman et al.³ among others. They concluded that a significant improvement in lift was achieved because the tunnel resonance could strongly enhance the outcomes, especially for some cases in which a large amplitude was required. Blevins⁵ investigated the influence of transversely acoustic waves on the shedding vortices about a circular cylinder in the wake. He found that the externally applied acoustics at the vortex shedding frequency could be well correlated with the shedding vortices along the span of the cylinder. The induced shedding frequency was shifted when the excitation frequency was applied near the natural shedding frequency of the vortices. He also pointed out that this entrainment was produced by the velocity induced from the sound wave rather than by the sound pressure. This result was confirmed by Hsiao et al.⁶ in the study of a flow passing a circular cylinder with acoustics "internally" emanated from the cylinder surface.

For the application of "internal" acoustic excitation about a stalled airfoil, Huang et al.⁴ studied the effect of the acoustics emanated from a narrow gap located in the midchord of a symmetrical airfoil. They found that the most effective excitation frequency for improving the airfoil performance was correlative with the vortex shedding frequency in the wake. For the detailed study of the internal acoustic excitation on the aerodynamic performance improvement about a high-AOA airfoil, Hsiao et al.⁷ found that the lift was increased and the drag was reduced as long as the excitation frequency was "locked-in" to the instability frequency of the separated shear layers and the excitation was located near the separation point of the boundary layers. Regarding these surveys, the enhancement of the shear layer instability by the unsteady forcing is a mechanism for the flow separation control.

However, as for the application of the internal acoustic excitation technique, the effectiveness of the forcing level on the aerodynamic performance about a high-AOA airfoil is not clear and remains to be studied. Especially, it is important to know how the forcing level plays the role in the improve-

Received Jan. 11, 1991; revision received July 20, 1991; accepted for publication Aug. 14, 1991. Copyright © 1991 by the American Institute of Aeronautics and Astronautics, Inc. All rights reserved.

*Senior Research Scientist, Aeronautical Research Laboratory.

†Professor, Institute of Aeronautics and Astronautics. Member AIAA.

‡Ph.D. Candidate, Institute of Aeronautics and Astronautics.

ment of the aerodynamic performance as compared to the effectiveness of the forcing frequency. This motivates us to examine jointly the dependence of the forcing level and the forcing frequency from this technique. The velocity fluctuation induced by the internally emanating acoustics at the slot exit will be used as an intensity parameter for the forcing level, which is measured when there is no wind blowing. When a larger amplitude forcing is applied, the internal excitation technique is similar to the unsteady base bleed (or the unsteady pulsing) method as used by Williams et al.^{8,9} in the sense that it creates a fluctuating region of fluid on the surface of the body. In addition, the analysis of the time-averaged pressure recovery on the upper surface of the airfoil will show that the reattachment of the separated shear layers and the length of the recirculated region are highly dependent on the forcing frequency. The flow visualization technique will also be carried out to investigate the vortical structure patterns over the airfoil.

Experimental Facilities

The experiments were conducted in a suction, open-typed wind tunnel with a 90×120 -cm test section. An airfoil model of 30 cm in chord with a NACA 63-018 cross section was used for velocity and pressure measurements. Fifty-eight surface pressure orifices were installed along the upper and lower surfaces of the airfoil in the midspan of the model. The acoustic fluctuations generated by a loudspeaker was funneled into the interior of the model and then ejected into the flowfield from a narrow slot of 0.6 mm in width at 1.25% chord from the leading edge, which is near the leading-edge separation point for the airfoil in the stalled condition. The loudspeaker was driven by a power amplifier with a variable-frequency function generator. The sound pressure level (SPL) was measured at the exit of the forcing slot by a CEL-254 digital sound level meter with no flow blowing. Throughout the measurements, the freestream velocity was kept at 15.5 m/s which is corresponding to the Reynolds number of 3.0×10^5 .

Information regarding the velocity fluctuations was acquired by a Dantec constant-temperature hot-wire anemometer. The frequency spectra were obtained by an Ono-sokki CF930 FFT analyzer. For the drag measurements, a Pitot tube mounted on a traversing mechanism was placed at two chords downstream from the trailing edge of the airfoil to investigate the momentum defect. The schematic diagram of the experimental setup is shown in Fig. 1. The more detail of the experimental apparatus and arrangements is referred to Hsiao et al.⁷

The flow visualization was carried out in a smoke tunnel with a 20×40 -cm test section. Another geometrically identical airfoil model of 12-cm chord with the corresponding Reynolds number of 1.0×10^4 was used in the visualization study. The smoke-wire technique is employed to visualize the flow developments over the model by photography and videotaped recording.

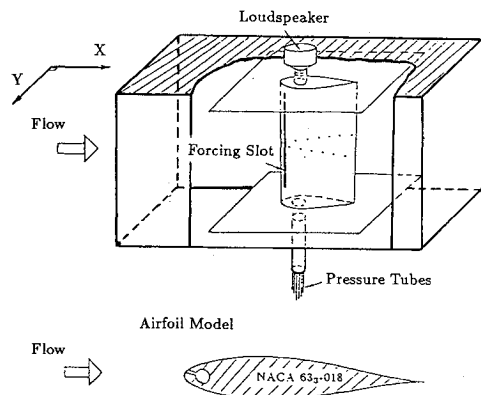


Fig. 1 Schematic diagram of the experimental setup.

Results and Discussion

Forcing Level as a Parameter

According to the papers surveyed,¹⁻⁷ the transverse velocity fluctuations induced by the acoustic excitation are effective in affecting the separated shear-layer properties than the induced pressure fluctuations. To overcome the impropriety that taking the sound pressure level (SPL) as a reference forcing intensity parameter, the velocity fluctuations measured right at the forcing slot exit are employed as a forcing level parameter in the study. Thus, the forcing level is first examined by monitoring the velocity fluctuations through a hot-wire anemometer when there is no freestream velocity. Figure 2 shows the typical time signals of the transversely forcing velocity fluctuations at some specific forcing frequencies. In order to avoid confusion in the reversed flowfield via the hot-wire measurements, the maximum value of the velocity fluctuations, denoted by u'_{\max} is used as a reference parameter for the excitation level. The level u'_{\max} is chosen between 2.5 and 10 m/s throughout the study. The corresponding SPL's measured at the slot exit are lower than 136 dB which is theoretically equivalent to the maximum acoustic velocity fluctuations of 0.29 m/s. It bears a small percentage comparable to the forcing disturbances. Thus, the velocity fluctuations created by the unsteady pulsing of the fluid around the slot are recognized to be the main disturbance sources. In other words, except enhancing the Kelvin-Helmholtz instability as proposed by Hsiao, et al.,⁷ the interaction between the forcing disturbances and the separated boundary layers is another possible mechanism to alter the flow behaviors.

When the airfoil is excited by a high frequency-sensitive loudspeaker at a constant, root-mean-squared (rms) driven voltage from the power amplifier with no freestream velocity, the induced u'_{\max} does not keep constant. Instead, it is very much dependent on the forcing frequency as plotted in Fig. 3a. The data in Fig. 3b depict the corresponding SPLs measured at the slot exit when the freestream velocity is still zero. The variation of the section lift coefficient with respect to the forcing frequency (Fig. 3c) also reveals its dependence on the given forcing level as well as the SPL. If forcing the stalled airfoil with another loudspeaker which is well responsive in the low frequency range, the result also demonstrates the dependence of the section lift coefficient on u'_{\max} as plotted in Fig. 4. It is lucid that u'_{\max} is an appropriate intensity parameter in examining the effects of the large amplitude ex-

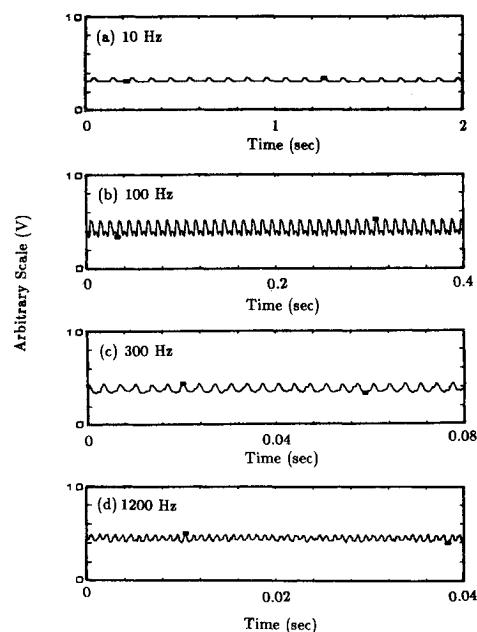


Fig. 2 Velocity fluctuation signals measured at the slot exit when there is no freestream velocity at constant driven voltage.

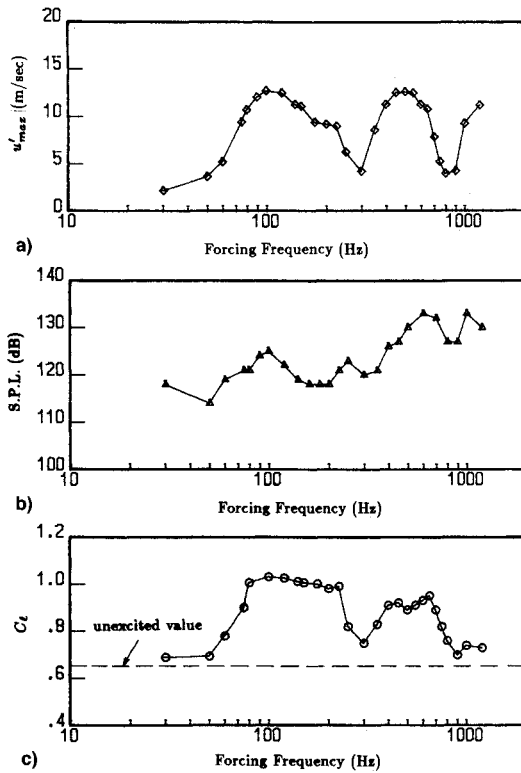


Fig. 3 a) Maximum velocity fluctuation; b) the corresponding sound pressure level at the slot exit; and c) the lift coefficient at constant driven voltage and AOA = 22 deg.

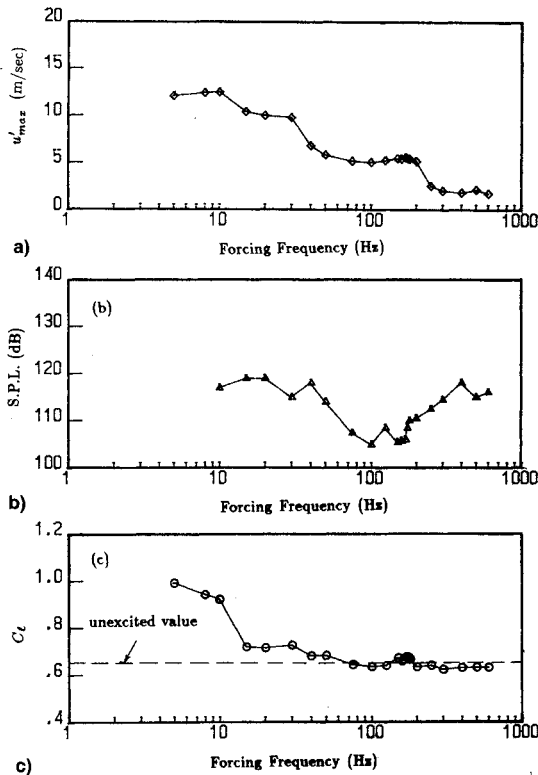


Fig. 4 a) Maximum velocity fluctuation; b) corresponding SPL; and c) lift coefficient at AOA = 22 deg and driven by a low-frequency-sensitive loudspeaker.

citation. In order to obtain a constant value of u'_{\max} for different frequency forcing, one must first calibrate the driven voltage setting of the power amplifier for each frequency. This is an important procedure before one proceeds to perform the experiments about the frequency effects on the airfoil performance under the same forcing levels.

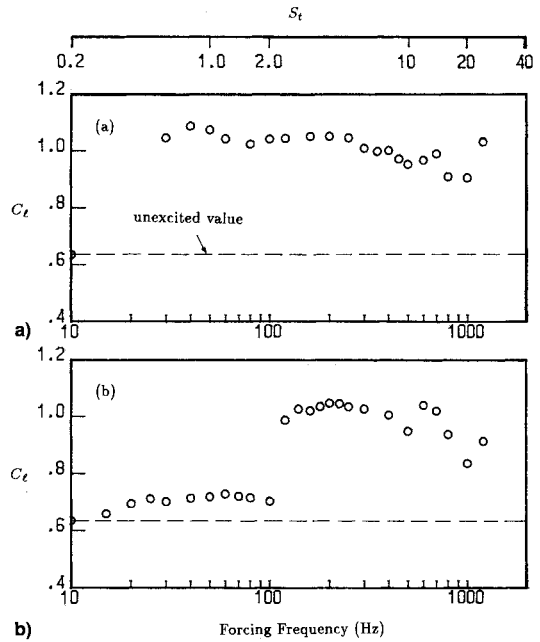


Fig. 5 Variation of section lift coefficient with forcing frequencies at AOA = 20 deg for a) $u'_{\max} = 3.7$ m/s, and b) $u'_{\max} = 2.5$ m/s.

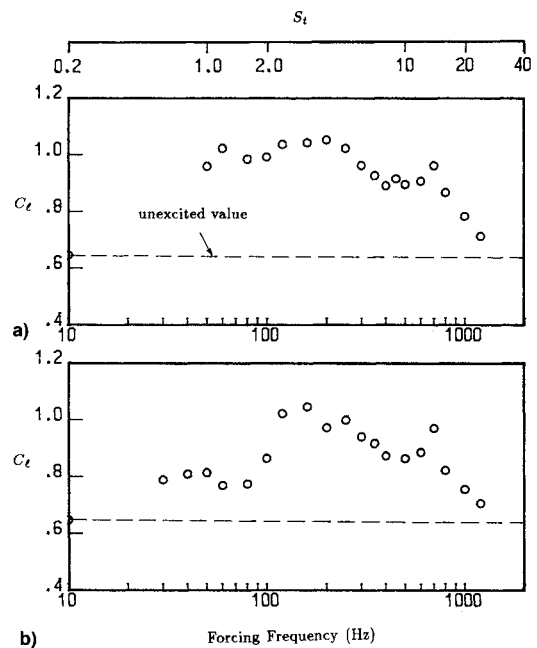


Fig. 6 Variation of section lift coefficient with forcing frequencies at AOA = 22 deg for a) $u'_{\max} = 5.3$ m/s, and b) $u'_{\max} = 4.2$ m/s.

Forcing Level Effects on Section Lift and Drag

It had been shown that the pressure distribution on the airfoil was quite sensitive to the forcing frequency of the acoustics applied.^{6,7} The effective forcing frequency for the present internal excitation technique is determined by examining the airfoil performance at various, constant forcing levels, u'_{\max} . Figs. 5, 6, and 7, respectively, depict the variations of the section lift coefficient with respect to the forcing frequency at various forcing levels for the angle of attack 20, 22, and 24 deg. The excited Strouhal number, $St = f_c C/U_\infty$, is also plotted for comparison. The section lifts are obtained by integrating the surface pressure distributions over the airfoil. For the lower-level forcing (see Figs. 5b and 6b), the increase in lift is more effective when the forcing frequency spans 120 Hz ($St = 2.4$) to 400 Hz ($St = 8$). This corresponds to the range of the separated shear layer instability frequency at the leading edge of the airfoil, which is about 250 Hz (St

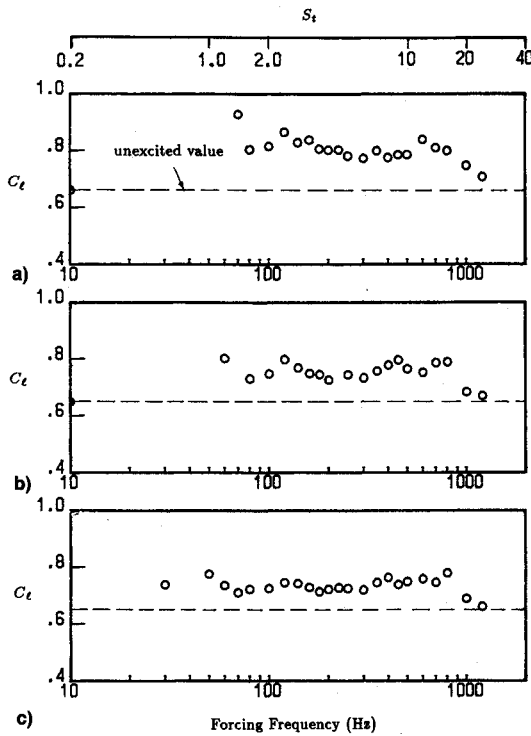


Fig. 7 Variation of section lift coefficient with forcing frequencies at AOA = 24 deg for a) $u'_{\max} = 10$ m/s; b) $u'_{\max} = 7.5$ m/s; and c) $u'_{\max} = 5.3$ m/s

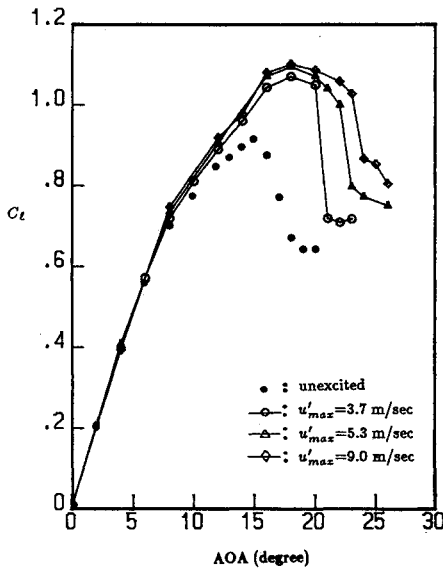


Fig. 8 Variation of section lift coefficient curve at the forcing frequency of 70 Hz ($St = 1.4$) for various forcing levels.

= 5). It confirms the conclusion by Hsiao et al.⁷ that the forcing is most effective when the forcing frequency is “locked-in” to the shear layer instability frequency. However, the effective forcing frequency extends a wider range when the forcing level increases to some higher values as shown in Figs. 5a and 6a. In addition, with the increase of the angle of attack to 24 deg as depicted in Fig. 7, a higher forcing level is needed in order to obtain a larger lift. Figs. 8 and 9, respectively, present the section lift coefficient curve with the angle of attack for various forcing levels at the forcing frequency of 70 Hz ($St = 1.4$) and 200 Hz ($St = 4$). The maximum lift coefficient and the stalled angle are significantly increased with the increase of the forcing level from no-forcing case to $u'_{\max} = 3.7$ m/s. Despite further increasing the forcing level to $u'_{\max} = 9.0$ m/s, the maximum lift improvement is gradually diminished. However, beyond the post-stalled region or the

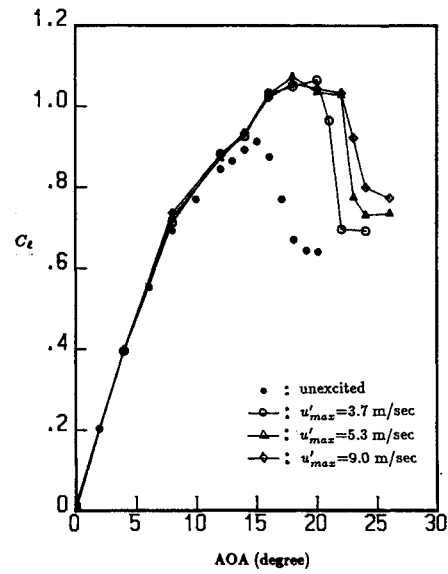


Fig. 9 Variation of section lift coefficient curve at the forcing frequency of 200 Hz ($St = 4$) for various forcing levels.

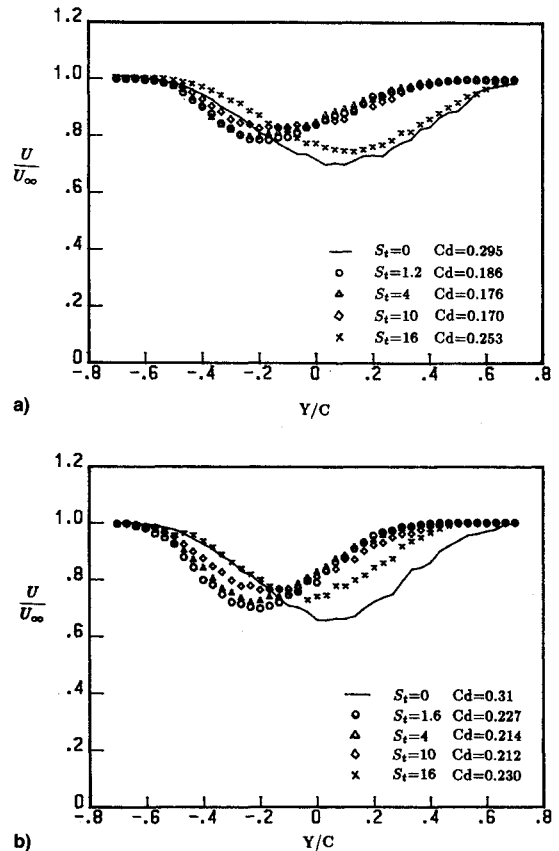


Fig. 10 Wake defect profiles with forcing frequencies of a) AOA = 18 deg and $u'_{\max} = 2.5$ m/s, and b) AOA = 20 deg and $u'_{\max} = 3.7$ m/s.

AOA greater than 20 deg, the section lift still remains augmented and the airfoil stall is delayed considerably. It demonstrates that the adequate higher level forcing would impact the separated flow behaviors to improve the airfoil performance. Moreover, because the momentum addition by the excitation is proportional to the square of the velocity fluctuation of the forcing, the effectiveness for the higher level excitation is due primarily to the additional momentum flux. This will be explained again in the subsequent sections.

Figure 10 shows the comparison of the wake defect profiles at two chords downstream from the trailing edge for the angles of attack of 18 and 20 deg when the flow is unexcited or excited

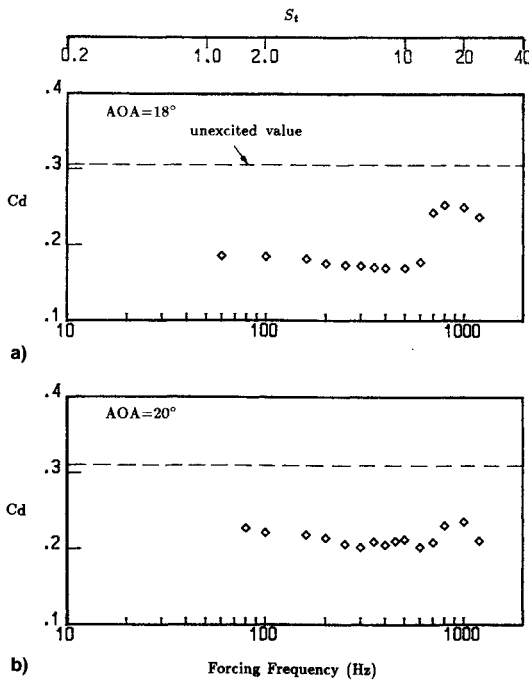


Fig. 11 Variation of section drag coefficient with forcing frequencies for a) $AOA = 18$ deg and $u'_{max} = 2.5$ m/s, and b) $AOA = 20$ deg and $u'_{max} = 3.7$ m/s.

with favorable frequencies and enough high-forcing level. The corresponding section drag coefficients are then calculated and collected in Fig. 11. Fig. 10 clearly demonstrates an achievement of the narrower wake region after the excitation, as compared to the flow without excitation. It seems due to the tendency of the boundary-layer reattachment to the wall surface, which would result in a significant reduction of the drag. This will be further substantiated by performing the flow visualization depicted in Fig. 14. By inspecting these results before and after excitation, it is found that the trend in the drag reduction is analogous to that of the lift increase. Thus, the double advantages, higher lift, and lower drag, will assure the higher value of the life-to-drag ratio and better aerodynamic performance after the introduction of the internal excitation technique.

Effect of Excitation on Pressure Distributions

The surface pressure distributions with and without excitation for the cases of the angle of attack 18, 20, and 22 deg are presented in Fig. 12. It clearly reveals that the upper surface pressure behaves quite different to the forcing frequency, and a suction peak area exists near the leading edge of the upper surface for all the excited cases. Thus, the lift produced should be increased as compared to the case without excitation. It is also found that, although the upper surface pressure is different, the integrated lifts are almost the same in the effective frequency range between 60 Hz ($St = 1.2$) and 600 Hz ($St = 10$) for the high-level forcing. When the flow is excited at the frequency of 200 Hz ($St = 4$) as shown in Figs. 12a and 12b or 300 Hz ($St = 6$) in Fig. 12c, which all correspond to the shear-layer instability frequency, the upper surface pressure recovered from the base pressure, $C_p = -1.0$, persists downstream almost to the mid-chord with a weaker suction peak formed in the front portion of the airfoil. However, when it is excited at 800 Hz ($St = 16$), the upper surface pressure acts to recover from the base pressure much earlier than the previous case at about 15% chord in Fig. 12a and 21% in Fig. 12b, but accompanying a steeper pressure spike. It demonstrates that the lower the forcing frequency is, the farther the pressure recovery moves. A detailed study is needed to examine the relationship between the forcing frequency and the pressure recovery point. For a

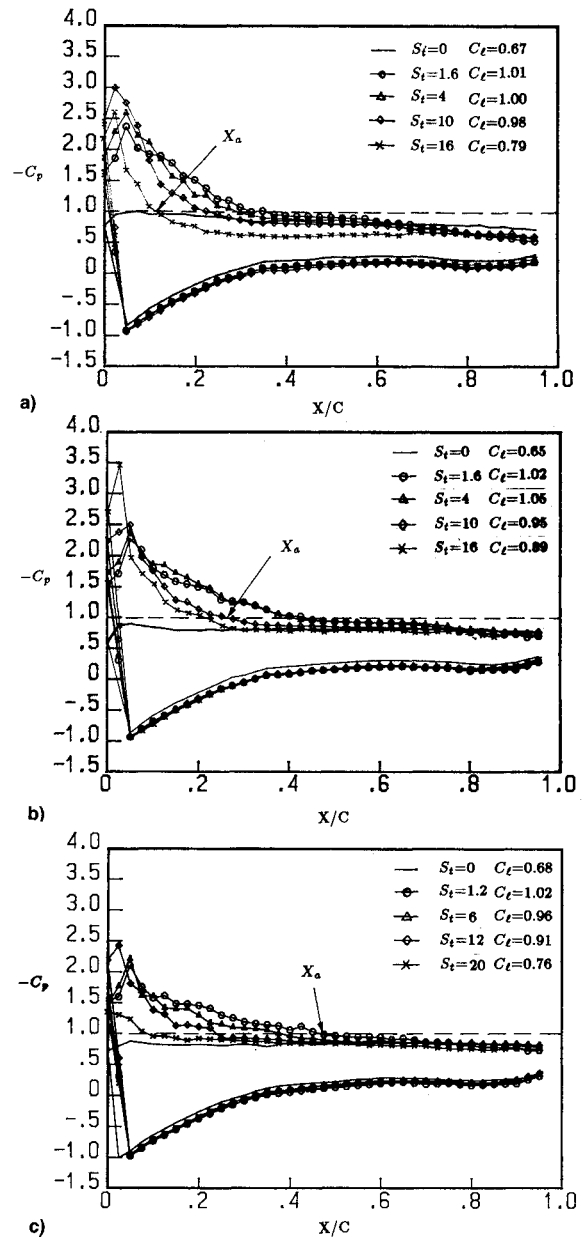


Fig. 12 Surface pressure distributions along the chord for various forcing frequencies at a) $AOA = 18$ deg and $u'_{max} = 2.5$ m/s; b) $AOA = 20$ deg and $u'_{max} = 3.7$ m/s; and c) $AOA = 22$ deg and $u'_{max} = 5.3$ m/s.

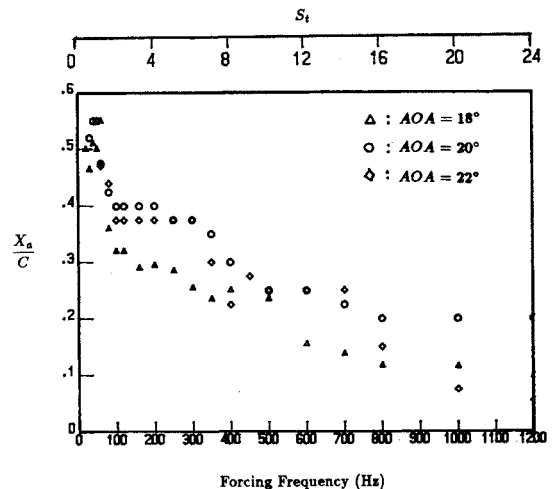


Fig. 13 Collection of the pressure recovery location with forcing frequencies at the same conditions of Fig. 12.

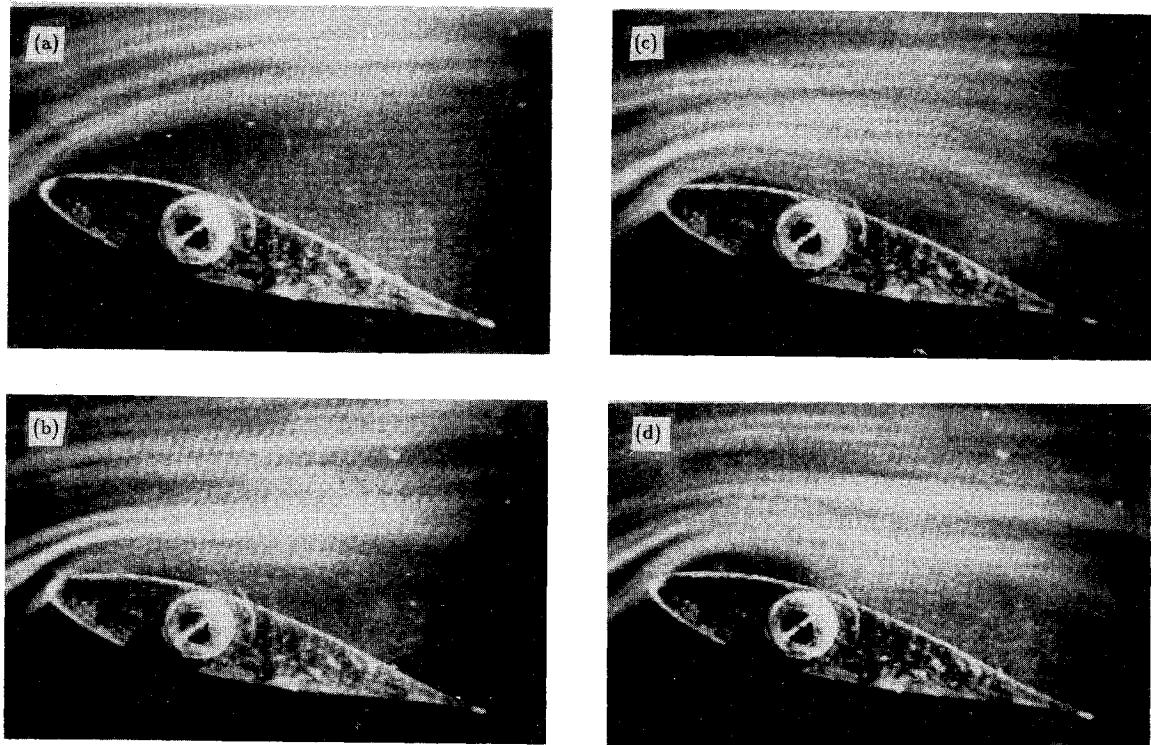


Fig. 14 Comparison of the flow patterns at AOA = 20 deg for the case: a) without excitation; b) with internal excitation at $St = 5$; c) $St = 3$; and d) $St = 1$ for $Re = 1.0 \times 10^4$.

given pressure profile, Montividas et al.¹⁰ proposed that the asymptotic pressure-recovery point X_a could serve as a measure of the reattachment control of the separated boundary layer. Hence, X_a is adopted as the length scale parameter and defined to be the distance measured from the leading edge of the airfoil to the position where the surface pressure reaches its base pressure. The results of X_a with the forcing frequency (and the Strouhal number) are collected in Fig. 13 for three angles of attack. For the low frequency forcing, in which the forcing frequency is less than half of the shear-layer instability frequency, 125 Hz, a sharp, low suction pressure area is developed immediately after the leading edge of the airfoil. In addition, a substantially longer pressure-recovery length is obtained. For the forcing around at the shear-layer instability frequency, 250 Hz ($St = 5$), the pressure-recovery length seems to keep constant for all the angles of attack tested. It then reduces its length with the increase of the forcing frequency. This is quite consistent with the result obtained by Montividas et al.¹⁰ in the study of vortex geometry behind pitching cylinders. This conclusion can also be confirmed in the flow visualization study.

Reasoning for the Acoustic Excitation

As far as the employment of a sufficient forcing level about the unsteady separated flows is concerned, the internal acoustic excitation method is regarded as a kind of active control.^{7,10} The vorticity-generation equation over the airfoil surface for an unsteady flow can be written as¹¹⁻¹³

$$\mu \left. \frac{\partial \Omega}{\partial y} \right|_s = - \frac{\partial U_s}{\partial t} - V_s \Omega - \frac{1}{\rho} \left. \frac{\partial P}{\partial x} \right|_s \quad (1)$$

In Eq. 1, the vorticity Ω generated, is balanced by the surface acceleration, $-\partial U_s/\partial t$, the transpiration through the wall, $-V_s \Omega$, and the local pressure gradient, $-\partial P/\partial x$. In the present study, the unsteady forcing effects by the internal excitation can be considered a combination of the local pressure gradient and the transpiration of the transverse perturbations via periodic blowing and suction processes. Therefore, the larger lift production as obtained in Figs. 8 and 9 can be

interpreted as a result of vorticity accumulation driven by an unsteady modulation. This argument is substantiated by performing the flow visualization study as depicted in Fig. 14 for the flow with and without excitation at the angle of attack 20 deg. The leading-edge separation is clearly revealed when the flow is unexcited (Fig. 14a). However, when the flow is excited at the shear-layer instability frequency of 50 Hz ($St = 5$) (Fig. 14b), the separated boundary layer is manifested to be reattached to the airfoil surface. This demonstrates that the locally introduced unsteady vorticity by the excitation is capable of manipulating the separated flow so as to produce the boundary-layer reattachment to the surface. The presence of a "closed" recirculating region over the airfoil provides the low pressure area on the upper surface with a high-lift generation. Consequently, the forcing effect is due primarily to the development of the periodically vortical disturbances created by the interaction between the unsteady forcing fluid and the flow around the airfoil. This result was also discussed by Ho¹² and Shih¹³ in the study of a stationary airfoil aerodynamics with periodically-varying freestream. In addition, Figs. 14c and 14d, respectively, demonstrate the presence of the recirculating regions for the lower forcing frequencies, 30 Hz ($St = 3$) and 10 Hz ($St = 1$). The flow patterns show that the reattachment length of the boundary layers has something to do with the forcing frequency. That is, the higher the forcing frequency is, the shorter the reattachment length will be. This also reconfirms the result in the measurements of the surface pressure recovery in Fig. 13.

Conclusion

The forcing level effects on improving the aerodynamic performance by using internal acoustic excitation are studied by means of the velocity and pressure measurements and the flow visualization. Both the sound pressure levels and the velocity fluctuations measured directly at the forcing slot are taken as the reference forcing parameters when there is no freestream velocity. Results indicate that, for the flow around the airfoil stalled angles tested, the "locked in" enhancement of the shear-layer instability by the unsteady forcing is a major mechanism when the forcing level is low. But for the higher

forcing level excitation, the transverse velocity fluctuation induced by the acoustics is also an important governing factor in modifying the flow properties. The forcing level significantly affects the aerodynamic properties, such as the lift coefficient, as compared to the forcing frequency that is mainly responsible for the lower level excitation. Moreover, the magnitude of the velocity fluctuations is very large as compared to the acoustic velocity disturbances. It means that the forcing effects are due primarily to the velocity fluctuations created by the unsteady pulsing of the fluid around the slot, especially when the forcing level is very high. Consequently, except when the Kelvin-Helmholtz instability is enhanced, the interaction between the forcing disturbances and the separated boundary layer is another mechanism to alter the flow behaviors.

From the results of the mean pressure distributions and the flow visualization, it is found that the locally introduced unsteady vorticity causes the separated boundary layer to be reattached to the surface. The pressure recovery length X_a depends upon the forcing frequency. In addition, the presence of a closed recirculated region provides the low pressures on the upper surface so that a higher lift is generated. Meanwhile, a narrower wake with a smaller velocity defect is obtained due to the boundary-layer reattachment after the excitation. This would result in a drag reduction correspondingly.

Acknowledgment

This work is supported by the National Science Council, Republic of China, under the Contract NSC 79-0210-D006-03.

References

¹Collins, F. G., and Zelenevitz, J., "Influence of Sound upon Separated Flow over Wings," *AIAA Journal*, Vol. 13, No. 3, 1975, pp.

408-410.

²Ahuja, K. K., and Burrin, R. H., "Control of Flow Separation by Sound," AIAA Paper 84-2298, Williamsburg, VA, Oct. 1984.

³Zaman, K. B. M. Q., Bar-Sever, A., and Mangalam, S. M., "Effect of Acoustic Excitation on the Flow Over a Low-Re Airfoil," *Journal of Fluid Mechanics*, Vol. 182, Sept. 1987, pp. 127-148.

⁴Huang, L. S., Bryant, T. D., and Maestrello, L., "The Effect of Acoustic Forcing on Trailing Edge Separation And Near Wake Development of An Airfoil," AIAA Paper 88-3531, Cincinnati, OH, July 1988.

⁵Blevins, R. D., "The Effect of Sound on Vortex Shedding from Cylinders," *Journal of Fluid Mechanics*, Vol. 161, Dec. 1985, pp. 217-237.

⁶Hsiao, F. B., Shyu, J. Y., Liu, C. F., and Shyu, R. N., "Experimental Study of Acoustically Excited Flow Over a Circular Cylinder," *Transport Phenomena in the Thermal Control*, edited by G. J. Hwang, Hemisphere, New York, 1989, pp. 537-546.

⁷Hsiao, F., Liu, C., and Shyu, J., "Control of Wall-Separated Flow by Internal Acoustic Excitation," *AIAA Journal*, Vol. 28, No. 8, 1990, pp. 1440-1446.

⁸Williams, D. R., and Amato, C. W., "Unsteady Pulsing of Cylinder Wakes," AIAA Paper 88-3532, Cincinnati, OH, July 1988.

⁹Williams, D. R., El-Khabiry, and Papzian, H., "Control of Asymmetric Vortices Around a Cone-Cylinder Geometry with Unsteady Base Bleed," AIAA Paper 89-1004, Tempe, AZ, March 1989.

¹⁰Montividas, R., Reisenhel, P., and Nagib, H., "The Scaling and Control of Vortex Geometry Behind Pitching Cylinders," AIAA Paper 89-1003, Tempe, AZ, March 1989.

¹¹Reynolds, W. C., and Carr, L. W., "Review of Unsteady, Driven, Separated Flows," AIAA Paper 85-0527, Boulder, CO, 1985.

¹²Ho, C. M., "Vortex Dynamics of Unsteady Flows," Invited lecture, 1st National Fluid Dynamics Congress, Cincinnati, OH, July 25-28, 1988.

¹³Shih, C., "Unsteady Aerodynamics of a Stationary Airfoil in a Periodically-Varying Free-Stream," Ph.D. Dissertation, Univ. of Southern California, Los Angeles, CA, Aug. 1988.

Recommended Reading from Progress in Astronautics and Aeronautics

Applied Computational Aerodynamics

P.A. Henne, editor

Leading industry engineers show applications of modern computational aerodynamics to aircraft design, emphasizing recent studies and developments. Applications treated range from classical airfoil studies to the aerodynamic evaluation of complete aircraft. Contains twenty-five chapters, in eight sections: History; Computational Aerodynamic Schemes; Airfoils, Wings, and Wing Bodies; High-Lift Systems; Propulsion Systems; Rotors; Complex Configurations; Forecast. Includes over 900 references and 650 graphs, illustrations, tables, and charts, plus 42 full-color plates.

1990, 925 pp, illus, Hardback, ISBN 0-930403-69-X

AIAA Members \$69.95, Nonmembers \$103.95

Order #: V-125 (830)

Place your order today! Call 1-800/682-AIAA



American Institute of Aeronautics and Astronautics
Publications Customer Service, 9 Jay Gould Ct., P.O. Box 753, Waldorf, MD 20604
Phone 301/645-5643, Dept. 415, FAX 301/843-0159

Sales Tax: CA residents, 8.25%; DC, 6%. For shipping and handling add \$4.75 for 1-4 books (call for rates for higher quantities). Orders under \$50.00 must be prepaid. Please allow 4 weeks for delivery. Prices are subject to change without notice. Returns will be accepted within 15 days.